JOURNAL OF GUIDANCE, CONTROL, AND DYNAMICS
Vol. 15, No. 5, September-October 1992

Effects of Deployment Rates and Librations on Tethered Payload Raising

K. Kumar* and R. Kumar†
Indian Institute of Technology, Kanpur, India
and
A. K. Misra‡
McGill University, Montreal, Quebec H3A 2K6, Canada

Raising a payload by deploying it from an orbiter on a long tether and then releasing it represents a rather important possible application of tethers involving significant fuel economy. Here, the effects of various deployment schemes as well as out-of-plane librations on tethered payload are studied. Orbital parameters are calculated for a payload released from a tethered system executing three-dimensional librational motion. This analysis accounts for the tether mass as well. For planar librations and circular prerelease orbits, a rule called the 7 + 4δ rule is obtained. Interestingly, contrary to intuition, an increase in deployment rate does not necessarily lead to an increase in apogee altitude of the released payload. Typical plots of the altitude gain vs deployment rate are presented showing peaks and valleys. These could be used to select the optimum deployment scheme for raising payloads to higher altitudes. Finally, attention is focused on the effect of roll motion on the resulting change of orbital plane.

Nomenclature

a, e = semimajor axis and eccentricity of the original orbit
a_2, e_2 = semimajor axis and eccentricity of the final orbit
K = Earth's gravitational constant
l_{max} = fully deployed tether length, $\epsilon = l_{max}/a$
l_t = instantaneous tether length
m = total mass of the system, $m_1 + m_2 + m_t$
m_e = equivalent mass of the system, $m[(m_1 + m_t/2)(m_2 + m_t/2)/m^2 - m_t/(6m)]$
m_{10} = initial orbiter mass before deployment begins
n = mean orbital rate, $\sqrt{K/a^3}$
R = magnitude of the position vector of the system center of mass
$\hat{R}$ = (R/a)
T, U = kinetic and potential energies, respectively
α, γ = pitch and roll angles, respectively
θ = time anomaly
λ = nondimensional instantaneous tether length during deployment, l_t/a
$\bar{\mu}$ = $(m_e/m) = [(\mu_1 + \mu_t/2)(\mu_2 + \mu_t/2) - \mu_t/6]$
μ_1 = $(m_1/m) = (m_{10} - \rho_t l_t)/m$
μ_2 = (m_2/m), $\mu_t = (m_t/m)$

Superscript

$'$ = $d(\ )/d(nt)$

Introduction

THE vast potential of tethered satellites is now well recognized. The 1990s could witness considerable space activity demonstrating specific tether applications. Raising a payload by deploying it upward from an orbiter on a long tether and then releasing it represents a rather important possible application involving significant fuel economy.

Bekey[1] and Bekey and Penzo[2] report that a tethered payload deployed upward and released will rise to a higher orbit with its perigee at the release point and its apogee on the opposite side of the Earth. If the release occurs in a nonlibrating situation with the tether along the local vertical, the altitude of the apogee is higher than that of the perigee by seven times the length of the tether. For a librating tethered satellite system, this payload altitude gain from perigee to apogee can increase to 14 times the tether length, whereas in the spinning systems considered, the corresponding figure could go up even further. Colombo et al.[3] have shown that tethered systems enable significant impulse savings for transfer missions from circular orbits. Their two-dimensional simulation assumes a massless tether and neglects tether dynamics, integrating only the equations of motion of the two end masses. On the other hand, McKinney and Tschirgi,[4] while considering Shuttle and space station-supported tethered satellite systems, account for tether mass along with gravity gradient in their analysis.

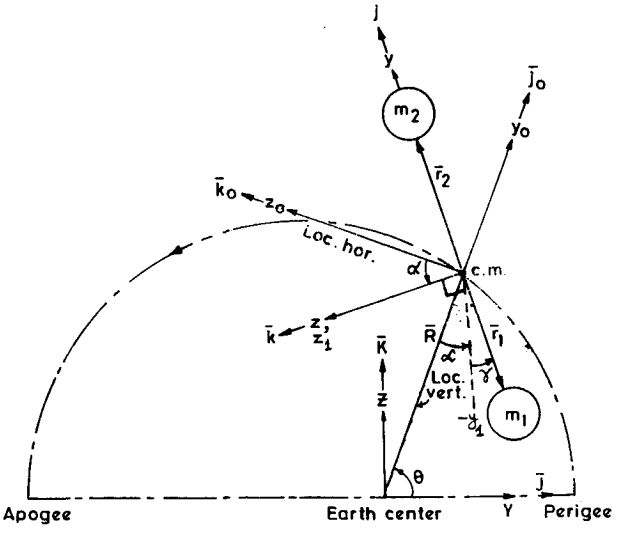

Fig. 1 Geometry of motion of a two-body tethered system.

Presented as Paper 89-454 at the AAS/AIAA Astrodynamics Specialist Conference, Stowe, VT, Aug. 7-10, 1989; received April 2, 1990; revision received Oct. 9, 1991; accepted for publication Nov. 23, 1991.

*Professor, Department of Aerospace Engineering. Associate Fellow AIAA.
†Graduate Student, Department of Aerospace Engineering.
‡Professor, Department of Mechanical Engineering. Associate Fellow AIAA.

More recently, Amier et al.[5] have focused attention on the effect of eccentricity of the starting orbit and prerelease three-dimensional attitude motion on the altitude reached by the payload after its disconnection. Kyroudis and Conway[6] have examined the use of an elliptically orbiting tethered dumbbell system for satellite transfer to geosynchronous altitude. In this two-dimensional analysis, several tether length and deployment rate combinations are considered to study their effect on δV savings. They conclude that elliptical orbits have certain advantages; they also note that, of the two deployment rates considered, the higher one leads to large δV savings.

Here, we systematically study the effects of various tether deployment schemes as well as the out-of-plane libration on raising of the payload orbit.

Formulation

A general two-body tethered system in a Keplerian orbit executing three-dimensional librational motion is considered (Fig. 1). The orbiter and the payload have masses m_1 and m_2, respectively. The tether has a mass ρ_t per unit length and a total mass of m_t. The instantaneous center of mass (c.m.) of the system is located by true anomaly θ and radial distance R. Denoted by $x_o y_o z_o$ is a rotating coordinate system with origin at the system c.m. such that the x_o axis is normal to the orbital plane, the axis y_o points along the local vertical, and the z_o axis is along the local horizontal completing the triad. The body coordinate frame xyz has an orientation such that the y axis is along the tether line.

The orientation of the tether-fixed frame xyz relative to the $x_o y_o z_o$ frame is described by the angles α and γ. The angle α denoting the rotation about the x_o axis is called the pitch angle; it transforms the axes x_o, y_o, z_o to x_1, y_1, z_1 axes. This is followed by a roll rotation γ about the z_1 axis that rotates x_1, y_1, z_1 to the tether axes x, y, z. The coordinate frame XYZ represents an inertial frame with origin at the Earth's mass center. The unit vectors $\bar{i}_o, \bar{j}_o, \bar{k}_o$ are along the x_o, y_o, z_o axes; $\bar{i}, \bar{j}, \bar{k}$ are along the x, y, z axes; and $\bar{I}, \bar{J}, \bar{K}$ denote units vectors along the X, Y, Z axes, respectively. The position vectors of masses m_1 and m_2 are denoted by $\bar{r}_1$ and $\bar{r}_2$, respectively. The analysis is based on the following assumptions:

1) The orbiter and the payload can be treated as point masses.

2) The only force taken into account is that due to the gravitational field of the spherical Earth. All other environmental effects are ignored.

3) The tether is rigid and remains straight. Its vibrations can be ignored.

For formulation of the system dynamics during deployment, the Lagrangian procedure is adopted. The expressions for the system's kinetic and potential energies obtained for this purpose can be written as follows:

$$T = (1/2)m(\dot{R}^2 + R^2\dot{\theta}^2) + (1/2)m_e l_t^2\left[(\dot{\theta}+\dot{\alpha})^2\cos^2\gamma + \dot{\gamma}^2\right] + (1/2)m_1\left[(m_2+m_t)/m\right]\dot{l}_t^2$$

$$U = -(Km/R) + \left[K/(2R^3)\right]m_e l_t^2(1 - 3\cos^2\alpha\cos^2\gamma) \quad (1)$$

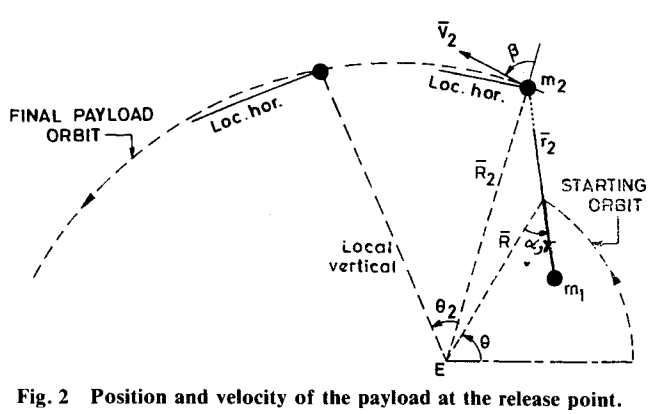

Fig. 2 Position and velocity of the payload at the release point.

It is now easy to apply a Lagrangian formulation to obtain the equations of motion governing the variation of the generalized coordinates R, θ, α, and γ in the following dimensionless form:

$$\hat{R}'' = \hat{R}\left[\theta'^2 - (1/\hat{R}^3)\{1 - (3/2)\bar{\mu}(\lambda\epsilon/\hat{R})^2(1 - 3\cos^2\alpha\cos^2\gamma)\}\right]$$

$$\theta'' = -2(\hat{R}'/\hat{R})\theta' + (3/2)\bar{\mu}(\lambda\epsilon/\hat{R})^2(1/\hat{R}^3)\sin 2\alpha\cos^2\gamma$$

$$\alpha'' = 2(\theta' + \alpha')\left[\gamma'\tan\gamma - (\mu_2 + \mu_t/2)(\mu_1/\bar{\mu})(\lambda'/\lambda)\right] + 2(\hat{R}'/\hat{R})\theta' - (3/2)(1/\hat{R}^3)\sin 2\alpha\left[1 + \bar{\mu}(\lambda\epsilon/\hat{R})^2\cos^2\gamma\right]$$

$$\gamma'' = -\left[2(\mu_1/\bar{\mu})(\mu_2 + \mu_t/2)(\lambda'/\lambda)\gamma' + (1/2)\sin 2\gamma \times \{(\theta' + \alpha')^2(3/\hat{R}^2)\cos^2\alpha\}\right] \quad (2)$$

Position and Velocity of the Payload at Release Point

The position and velocity vectors for the payload mass m_2 at the instant of release define its orbit when it is disconnected. Hence, these vectors (which we denote by $\bar{R}_2$ and $\bar{V}_2$, respectively) should be obtained in terms of R θ, α, γ, and their derivatives. This in turn requires the X, Y, Z components of the system angular velocity vector $\bar{\omega}$, which can easily be obtained as follows:

$$\bar{\omega} = \begin{Bmatrix}\omega_X\\ \omega_Y\\ \omega_Z\end{Bmatrix} = \begin{Bmatrix}\dot{\theta}+\dot{\alpha}\\ -\dot{\gamma}\sin(\theta+\alpha)\\ \dot{\gamma}\cos(\theta+\alpha)\end{Bmatrix} \quad (3)$$

Noting that

$$\bar{R}_2 = \bar{R} + \bar{r}_2, \qquad \dot{\bar{R}}_2 = \dot{\bar{R}} + \dot{\bar{r}} = \dot{\bar{R}} + \bar{\omega}\times\bar{r}_2 \quad (4)$$

where $\bar{r}_2$ is the position vector of the payload with respect to the c.m., it can be shown that

$$\bar{R}_2 = \begin{Bmatrix}-r_2\sin\gamma\\ R\cos\theta + r_2\cos\gamma\cos(\theta+\alpha)\\ R\sin\theta + r_2\cos\gamma\sin(\theta+\alpha)\end{Bmatrix} \equiv \begin{Bmatrix}X_2\\ Y_2\\ Z_2\end{Bmatrix} \quad (5)$$

$$\bar{V}_2 = \begin{Bmatrix}-r_2\dot{\gamma}\cos\gamma\\ \dot{R}\cos\theta - R\dot{\theta}\sin\theta - r_2(\dot{\theta}+\dot{\alpha})\cos\gamma\sin(\theta+\alpha)\\ -r_2\dot{\gamma}\sin\gamma\cos(\theta+\alpha)\\ \dot{R}\sin\theta + R\dot{\theta}\cos\theta + r_2(\dot{\theta}+\dot{\alpha})\cos\gamma\cos(\theta+\alpha)\\ -r_2\dot{\gamma}\sin(\theta+\alpha)\end{Bmatrix} \equiv \begin{Bmatrix}V_{2X}\\ V_{2Y}\\ V_{2Z}\end{Bmatrix} \quad (6)$$

Thus,

$$R_2 = \left[R^2 + r_2^2 + 2Rr_2\cos\alpha\cos\gamma\right]^{1/2} \quad (7)$$

$$V_2 = \left[\dot{R}^2 + R^2\dot{\theta}^2 + r_2^2\dot{\gamma}^2 + r_2^2(\dot{\theta}+\dot{\alpha})^2\cos^2\gamma - 2\dot{R}r_2\{\dot{\gamma}\sin\gamma\cos\alpha + (\dot{\theta}+\dot{\alpha})\cos\gamma\sin\alpha\} + 2Rr_2\dot{\theta}\{-\dot{\gamma}\sin\gamma\sin\alpha + (\dot{\theta}+\dot{\alpha})\cos\gamma\cos\alpha\}\right]^{1/2} \quad (8)$$

where

$$r_2 = \left[(m_1 + m_t/2)/m\right]l_{\max}$$

It may be noted that $\dot{l}_t$ does not appear in the velocity expression. This is because it is assumed that the reel-out/reel-in operations have ended prior to the release of the payload.

Orbital Elements of the Payload After Release

Once the expressions for the position vector and velocity of the payload have been expressed in terms of the pitch and roll motion of the tethered system, the orbital elements of the payload after release can be determined assuming that it executes standard central force motion.

Let β_2 denote the angle between the radial line and the velocity vector of the payload as shown in Fig. 2, that is, the heading angle is $\pi/2-\beta_2$. Then,

$$\cos\beta_2 = (\bar{R}_2\cdot\bar{V}_2)/(R_2V_2) \tag{9}$$

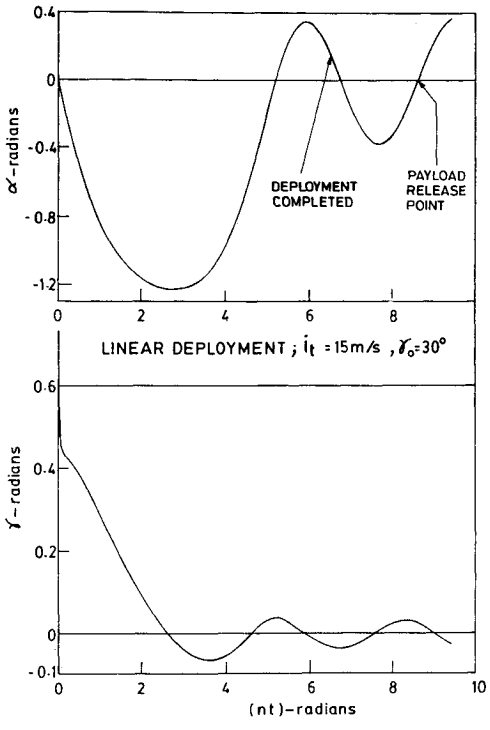

a)

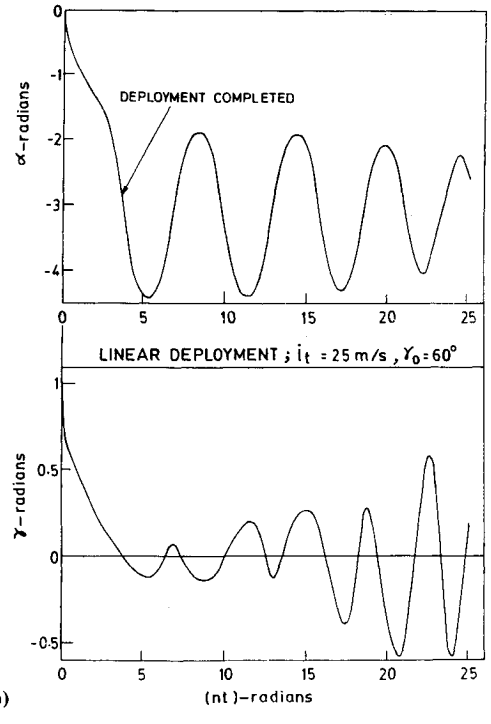

b)

Fig. 3 Typical pitch and roll variations during uniform deployment and after deployment: a) $\dot{l}_t = 15$ m/s, $\gamma_o = 30$ deg; b) $\dot{l}_t = 25$ m/s, $\gamma_o = 60$ deg.

The semimajor axis and eccentricity of the orbit of the payload after its release can now be written as

$$a_2 = R_2/\left[2-(R_2V_2^2/K)\right] \tag{10}$$

$$e_2^2 = \left[(R_2V_2^2/K)-1\right]^2 + (R_2V_2^2/K)(2-R_2V_2^2/K)\cos^2\beta_2 \tag{11}$$

The gain in apogee height is given by

$$\Delta R_{a_2} = R_{a_2} - R_a$$
$$= a_2(1+e_2) - R_a \tag{12}$$

where R_a is the apogee height of the original orbit.

In the presence of out-of-plane librations, the orbital plane of the released payload differs from that of the original orbital plane, i.e., Y-Z plane. This plane change can be calculated as follows. The angular momentum per unit mass is given by

$$\bar{h}_2 = \bar{R}_2\times\bar{V}_2 = (Y_2V_{2Z}-Z_2V_{2Y})\bar{I} + (Z_2V_{2X}-X_2V_{2Z})\bar{J}$$
$$+ (X_2V_{2Y}-Y_2V_{2X})\bar{K}$$
$$= h_X\bar{I} + h_Y\bar{J} + h_Z\bar{K} \tag{13}$$

If i_2 is the inclination of the new orbit to the original orbit, then

$$\cos i_2 = h_X/|\bar{h}_2| \tag{14}$$

An alternate expression that is more convenient for calculating i_2 is

$$\tan i_2 = (h_Y^2+h_Z^2)^{1/2}/h_X$$
$$= \left[(Z_2V_{2X}-X_2V_{2Z})^2+(X_2V_{2Y}-Y_2V_{2X})^2\right]^{1/2}$$
$$/(Y_2V_{2Z}-Z_2V_{2Y}) \tag{15}$$

The expressions for X_2, V_{2X}, etc., are obtained from Eqs. (5) and (6).

Schemes for Tether Deployment and Numerical Computation

One of the objectives of this investigation is to study the effect of various tether deployment schemes on gain in apogee altitude as well as the change in orbital inclination. The deployment schemes considered are as follows.

Uniform deployment scheme:

$$l_t = l_{to} + \dot{l}_t t, \qquad \dot{l}_t = b = \text{const} \tag{16}$$

Exponential deployment scheme:

$$l_t = l_{to}\exp(ct) \tag{17}$$

Here, c is chosen so as to ensure the same deployment time for the uniform and exponential schemes and is given by

$$c = \left[b/(l_{\max}-l_{to})\right]\ln(l_{\max}/l_{to}) \tag{18}$$

The set of four nonlinear, nonautonomous differential equations [Eqs. (2)] is integrated numerically. The integration continues beyond the end of deployment with $\dot{l}=0$ until the point of payload release, which occurs at the position where the pitch rate is a maximum, i.e., the payload is aligned with the local vertical within a tolerance of 5×10^{-4} rad. Next, Eqs. (5) and (6) are utilized to obtain the position and velocity vectors of the payload at release, which in turn enable computation of its subsequent final orbit. It is now easy to calculate the payload apogee gain subsequent to the tether release.

Likewise, changes in the inclination of the orbital plane resulting from initial roll disturbance can also be computed using Eqs. (13) and (15).

7+4δ Rule

Consider the special case when the orbit is circular and the out-of-plane librations are absent. Substituting $\dot{R}=\gamma=\dot{\gamma}=0$ and $\dot{\theta}=n$ in Eqs. (7) and (8), one obtains

$$R_2=\left[R^2+r_2^2+2Rr_2\cos\alpha\right]^{1/2} \tag{19}$$

$$V_2=\left[R^2n^2+r_2^2(n+\dot{\alpha})^2+2Rr_2n(n+\dot{\alpha})\cos\alpha\right]^{1/2} \tag{20}$$

Furthermore, using Eqs. (5), (6), and (9), one obtains

$$\cos\beta_2=-Rr_2\dot{\alpha}\sin\alpha/R_2V_2 \tag{21}$$

For optimum results, $\bar{R}_2$ and $\bar{V}_2$ must be perpendicular, i.e., $\cos\beta_2=0$, implying that α must be equal to zero. Thus, the release of the payload must take place when the tether is aligned with the local vertical, during its libration. Let the corresponding value of $\dot{\alpha}$ be $n\delta$, where δ is the ratio of the pitch rate at the local vertical position to the orbital rate. Equations (19) and (20) then yield

$$R_2=R+r_2 \tag{22}$$

$$V_2=n\left[R+r_2(1+\delta)\right] \tag{23}$$

The semimajor axis and eccentricity of the orbit of the payload after the tether has been disconnected are given by

$$a_2=(R+r_2)\Big/\left\{2-(R+r_2)n^2\left[R+r_2(1+\delta)\right]^2/K\right\} \tag{24}$$

$$e_2=\left\{(R+r_2)n^2\left[R+r_2(1+\delta)\right]^2/K\right\}-1 \tag{25}$$

Noting that for a circular orbit, $n^2=K/R^3$, one obtains, after some algebra,

$$R_{a_2}=a_2(1+e_2)$$
$$=R(1+\hat{r}_2)^2\left[1+\hat{r}_2(1+\delta)\right]^2\Big/\left\{2-(1+\hat{r}_2)\left[1+\hat{r}_2(1+\delta)\right]^2\right\} \tag{26}$$

where

$$\hat{r}_2=r_2/R \tag{27}$$

It may be recalled that r_2 is the distance of the payload from the system center of mass, i.e., $r_2<\ell$; thus $r_2\ll R$ and $\hat{r}_2\ll 1$. One can thus expand the right-hand side of Eqs. (26) using the binomial theorem to obtain

$$R_{a_2}=R\left[1+(7+4\delta)\hat{r}_2\right] \tag{28}$$

Hence, the apogee altitude gain is given by

$$\Delta R_{a_2}=R_{a_2}-R=(7+4\delta)r_2 \tag{29}$$

Equation (29) holds for both swinging systems as well as spinning systems. Thus, in the presence of in-plane libration or spin, the seven-times rule mentioned by Bekey and Penzo[2] is modified to the seven-plus-four-delta rule.

It may be pointed out that r_2 is equal to $(\mu_1+\mu_t/2)\ell$ where μ_1 and μ_t are the mass ratios defined in the Nomenclature. In many practical situations, the masses of the payload and tether are likely to be small compared to the orbiter mass, in which case $r_2\approx\ell$.

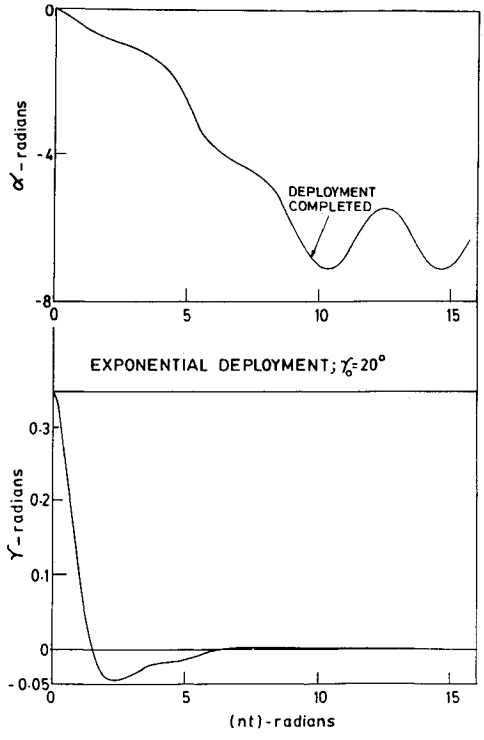

Fig. 4 Typical plot showing continual pitching drift during exponential deployment with large $\dot{\ell}_t/\ell_t$.

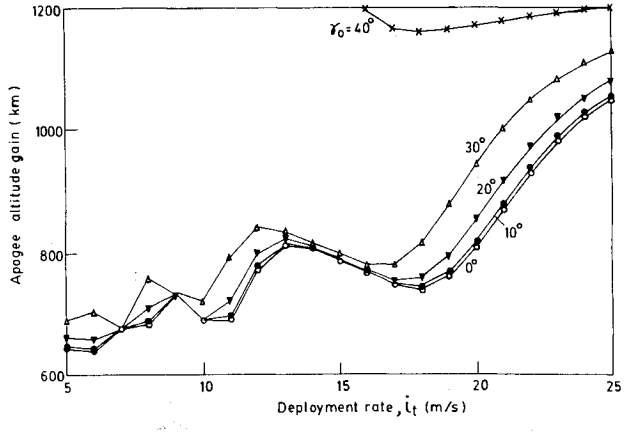

Fig. 5 Typical variation of gain in apogee altitude as influenced by the uniform deployment rate.

Table 1 Variation of apogee height gain and semimajor axis increase with eccentricity

e	ΔR_{a_2}, km	Δa, km
0	987	536
0.01	1,051	536
0.05	1,630	546
0.10	2,866	721
0.50	18,511	2,487

Numerical Results and Discussion

To start with, numerical results were obtained for the case when the initial orbit is circular. The following system parameters were used: $m_1=86{,}000$ Kg; $m_2=23{,}100$ Kg; $m_t=500$ Kg; $l_{to}=$ initial length of the tether $=10$ m; $l_{\max}=$ the maximum tether length $=100$ km; and $R=$ radius of the circular orbit $=7516$ km. The tethered system is assumed to enter its nominal circular orbit with the following initial conditions:

$$\alpha_o=\dot{\alpha}_o=\dot{\gamma}_o=0$$

whereas γ_o has been allowed to vary to study the effect of the initial roll angle.

The deployment scheme has negligible effect on the prerelease orbit; however, it has significant effects on the pitch and roll response as shown in Fig. 3 for the uniform case. The payload mass m_2 is disconnected as soon as it attains the maximum pitch rate with the tether aligned along the local vertical after the deployment has been completed (see Fig. 3a, which shows the release point at $\alpha=0$, $\dot{\alpha}=+ve$). Interestingly, on one hand, the deployment excites the pitching librations, whereas on the other hand, the out-of-plane libration, which is present by virtue of the initial roll disturbance, exhibits rapid decay. This damping phenomenon can be explained through the simplified linearized version of the nonlinear roll equation in Eqs. (2) in which the deployment rate term plays the role of viscous damping. In the case considered in Fig. 3b, the linear deployment, which is quite high, leads to pitching instability. In view of this large pitching motion, one can expect this deployment scheme to lead to large apogee altitude gain.

It is interesting to note that, during exponential deployment shown in Fig. 4, the magnitude of pitch angle α increases monotonically with time. This may be attributed to the fact that, if $\dot{\ell}_t/n\ell_t>0.75$, exponential deployment is unstable.[7] Here, n is the mean orbital rate. In the postdeployment phase, the amplitude of α, and hence $\dot{\alpha}$, continues to remain large, due to the virtual absence of damping in the system. Hence, such deployments can be useful for the intended purpose. The release should occur at $\alpha=2\pi$ after the completion of deployment.

Next, the uniform deployment case is examined in detail to study the apogee altitude gain of the upper mass m_2 as affected by the deployment rates (Fig. 5). It may be mentioned here that Kyroudis and Conway[6] had observed an increase in apogee altitude of the payload with deployment rate. Although this is true in a broad sense, an increase in deployment rate does not necessarily lead to an increase in apogee altitude of the payload after release. Instead, the plots are characterized by the presence of peaks and valleys. It is not surprising that the shape of the curves in Fig. 5 is similar to the one plotting the final pitch amplitude vs deployment rate in the work of von Flotow and Williamson.[8] In view of Eq. (29), the altitude gain depends on the maximum pitch rate δ, which in turn depends on the amplitude of pitch librations after deployment. If $\gamma=0$, it is possible to obtain an analytical expression for the amplitude of pitch oscillations for the uniform deployment case. On the basis of that, it can be shown that δ is a maximum or minimum when $\dot{\ell}_t=\sqrt{3}n\ell_{\max}/\pi k$, where k is an integer. For the parameters considered here, it becomes $\dot{\ell}_t=(54/k)$ m/s. On the basis of Fig. 5, it is clear that one should choose a value of deployment rate such that the apogee altitude gain does not hit a valley.

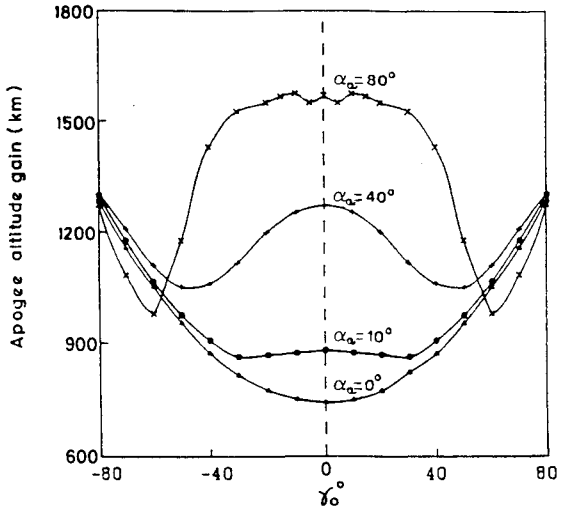

Fig. 6 Variation of the apogee height gain with pitch and roll amplitudes.

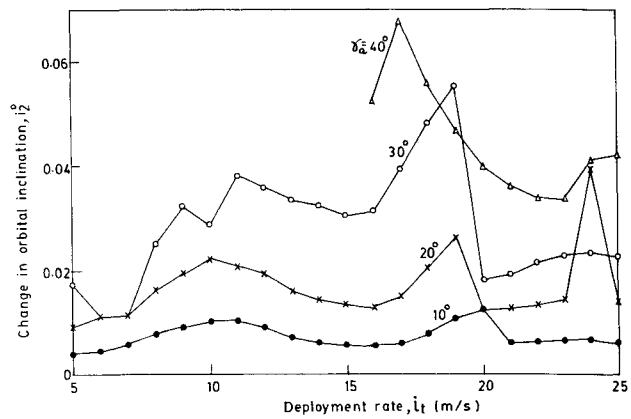

Fig. 7 Typical changes in the inclination of the orbital plane as influenced by γ_a (uniform deployment).

The effects of three-dimensional librational motion of the tethered system on the apogee altitude gain are shown in Fig. 6. In this figure, α_a and γ_a stand for the amplitudes of pitch and roll oscillations in the postdeployment phase. It may be noted that, if the amplitude of in-plane pitch oscillation is small, then roll motion helps as far as apogee height increase is concerned. However, if α_a is large (say 80 deg), then the addition of roll motion may actually reduce the apogee altitude. Of course, in all cases there is a change in the orbital plane.

Attention is now focused on the effect of the initial roll angle on the resulting change in the inclination of the payload orbit after release (Fig. 7). The plots show this effect over a range of constant deployment rates for several cases of nonzero initial roll angles but with zero roll rate. The changes in orientation of the payload orbit after release are found to be rather small, however.

Finally, a set of numerical results were obtained for the case when the prerelease orbit is elliptical. The parameters used are $m_1=10^5$ kg, $m_2=500$ kg, $m_t=500$ kg, and $\ell_{\max}=100$ kg. The perigee altitude of the initial orbit was assumed to be 6818 km, and the eccentricity was varied from 0.0 to 0.5. The maximum nondimensional pitch rate was assumed as 0.1. The gain in the apogee altitude and the change in the semimajor axis are shown in Table 1. It may be noted that a larger altitude gain can result for higher eccentricity. This is consistent with the observations of Kyroudis and Conway[6] that elliptic orbits have an advantage over circular orbits for tethered payload release.

Concluding Remarks

The investigation reported here considers a general two-body dumbbell system in an elliptic orbit executing three-dimensional librational motion during deployment. The analysis accounts for mass of the tether; however, its transverse vibrations have been ignored. For illustrations, the case of a specific 100-km-long tethered system in either a circular or elliptic orbit has been considered. The study shows that, contrary to the intuition, an increase in deployment rate does not necessarily lead to an increase in apogee altitude of the payload after its release. The plots of the apogee altitude gain vs deployment rate exhibit clear peaks and valleys. These could be used to select a suitable deployment rate, from the practically feasible ones, for raising payloads to higher altitudes. Finally, the changes in the orientation of the payload orbit after its release, subsequent to uniform deployment starting with nonzero initial roll angles, are rather small and, hence, are unlikely to have any significant impact on such missions.

References

[1]Bekey, I., "Tethers Open New Space Options," *Astronautics and Aeronautics,* Vol. 21, No. 4, 1983, pp. 33–40.

[2]Bekey, I., and Penzo, P. A., "Tether Propulsion," *Aerospace America,* Vol. 24, No. 7, 1986, pp. 40–43.

[3]Colombo, G., Martinez-Sanchez, M., and Arnold, D., "Use of Tethers for Payload Orbit Transfer," Smithsonian Astrophysical Observatory, NAS 8-33691, Cambridge, MA, March 1982.

[4]McKinney, L. E., and Tschirgi, J. M., "Tethers Deployed SSUS-A (Spin Stabilized Upper Stage)," McDonnell Douglas Corp., NAS8-33842, Huntington Beach, CA, April 1984.

[5]Amier, Z. E., Misra, A. K., and Modi, V. J., "Effect of Attitude Dynamics on Tether Propulsion," *Proceedings of the NASA/PSN/AIAA Conference on Tethers in Space,* Venice, Italy, Oct. 1987, pp. 468–476.

[6]Kyroudis, G. A., and Conway, B. A., "Advantages of Tether Release of Satellites from Elliptic Orbits," *Journal of Guidance, Control, and Dynamics,* Vol. 11, No. 5, 1988, pp. 441–448.

[7]Misra, A. K., and Modi, V. J., "A Survey on the Dynamics and Control of Tethered Satellite Systems," *Advances in the Astronautical Sciences,* Vol. 62, 1986, pp. 667–719.

[8]von Flotow, A. H., and Williamson, P. R., "Deployment of a Tethered Plasma Diagnostics Satellite into a Low Earth Orbit," *Journal of the Astronautical Sciences,* Vol. 34, No. 1, 1986, pp. 65–90.